



ISSN: 2579-1184(Print)

**FUPRE Journal**  
of

Scientific and Industrial Research

ISSN: 2578-1129 (Online)

<https://fupre.edu.ng/journal>

## Assessment of Saltwater Intrusion into Coastal Aquifer using Electrical Resistivity Method: A Case Study of Ojo, Lagos State

Adeogun, O. Y.<sup>2,\*</sup> , Adegbola, R. B.<sup>1</sup> Eze, P. O.<sup>1</sup> , Ishola, K. S.<sup>2</sup> , Ogbeide, O. I.<sup>1</sup>,  
Alli, S. A.<sup>2</sup>

<sup>1</sup>Department of Physics, Lagos State University, Ojo, Lagos, Nigeria

<sup>2</sup>Department of Geosciences, University of Lagos, Akoka, Lagos, Nigeria

### ARTICLE INFO

Received: 07/08/2022

Accepted: 19/10/2022

### Keywords

Coastline, Saltwater intrusion, 2D Electrical resistivity imaging, Coastal aquifer, Geoelectric sections

### ABSTRACT

The migration of saline water into freshwater aquifers is known as saltwater intrusion, and it has long been a source of concern around the world. Coastal regions are home to about 60% of the world's population. It is critical to assess the impact of saltwater intrusion on groundwater potential along the Ojo shoreline in Lagos State in order to determine suitable location for groundwater extraction for domestic use. The 2D Electrical Resistivity Imaging (ERI) survey was complemented with twenty Vertical Electrical Sounding (VES) measurements conducted along four traverses (TR) covering a total spread length (AB/2) of 120 m. The sand delineated in the second layer of the 2D electrical resistivity images across TR (1, 3 and 4) with low resistivity response revealed the lateral and vertical extent of contamination. The 2D results also coincided with the anomaly observed in the VES results. The sand identified in the second and third layers along TR1 (VES 3 and 4), TR3 (VES 11–13) and TR4 (VES 18 and 19) with associated low resistivity values of range 1.3–10.6  $\Omega\text{m}$  at depth range 0.5–44 m showed the relative degree of saltwater intrusion when compared to the identified sand in TR2 away from the Beachline. However, a probable confined freshwater aquifer with resistivity range 100.5–278  $\Omega\text{m}$  for VES (1 and 2) along TR1, VES (16) along TR4 at depth 30 m and VES (8) along TR2 at depth range 14–32 m was identified at fourth and fifth geoelectric layers. This study has shown the possible infiltration of salt water into the groundwater along the coastline. Hence, it is essential to monitor the saline contamination to preserve the quality of groundwater in such areas.

## 1. INTRODUCTION

Saltwater intrusion occurs due to the induced flow of seawater into the freshwater aquifers which might have been caused by exploitation of groundwater around the coastal region (Al-Barwani and Helmi 2006; Werner and Simmons, 2009; Oladipo et al., 2014; Herbert et al., 2015; Bellafigore et al., 2021). Great percentage of the world's population are said to be living within the ocean shoreline (Richter and Kreitler, 1993;

Tomaszkiewicz et al., 2014). The coastal region only takes up about 10% of the earth surface (Hinrichsen et al., 2007). So, the pressure on coastal aquifers is increasing, leading to greater risk of saltwater intrusion. There is need to monitor the level of saltwater intrusion on groundwater. Geophysical methods such as electrical, electromagnetic, induced polarization and borehole logging among others have been used and are still relevant to identify and monitor saltwater intrusion (Adepelumi et al., 2008; Satriani et al., 2012; Ayolabi et al., 2013; Cong-Thi et al.,

Corresponding author: [kemmyadesanya@gmail.com](mailto:kemmyadesanya@gmail.com)

DIO

@ Scientific Information, Documentation and Publishing Office at FUPRE Journal

2021). Electrical method is the preferred method because it is cheap, non-invasive, fast and provides good electrical resistivity contrast between

the target of interest and the host material (Adeogun et al., 2019). Khalil, 2006 used geoelectric resistivity sounding to delineate saltwater intrusion in the Abu Zenima area, west Sinai, Egypt likewise Adeoti et al., (2010), used geoelectrical methods to map saline water intrusion into freshwater aquifers at Oniru, Lagos State. Cong-Thi et al., 2021 used electrical resistivity tomography to map the extent of saltwater intrusion around Luy river at BinhThuan Vietnam. Most often, freshwater aquifer tends to have high resistivity values compared with coastal region associated with low resistivity values which could indicate presence of saltwater (Adeoti et al., 2010; Manivannan and Elango, 2019). Excess groundwater pumping from coastal aquifers than the rate of recharge and density difference between the saline water and freshwater in the aquifer is a major factor causing saltwater intrusion (Adeoti et al., 2010; Robinson et al., 2016). Lagos state for instance can easily be accessed through road, rail, and seaports. Like every other coastal belt, it experiences various degrees of saline water intrusion, especially along the coastal line because of its reliance on the groundwater exploration to support the inadequate water supply from pipe borne water (Adeoti et al. 2010). Saltwater intrusion has been a major threat to the coastal freshwater resources at Ojo, rendering

groundwater non-potable and causing well abandonment or requiring costly treatment systems. This informed the application of electrical resistivity method to map saltwater intrusion level into the freshwater aquifer along the beachline Ojo, Lagos so as to determine the most suitable location for groundwater extraction in the study area to meet the growing community demand.

The Beachline is located along the coastline in Ojo, Lagos state, Nigeria (Figure 1). It is about 14.3 km away from Lagos State University and it is situated on the coastal margin of Lagos state. Lagos state is a zone of coastal creeks and lagoons (Adepelumi et al., 2009), a region underlain by sedimentary deposits of the coastal plain sand also known as the Benin formation (Oteri and Atolabge, 2003). The coastal plain sand is composed essentially of sand, silt and clay. The coastal plains sand is the main aquifer in Lagos that is exploited through hand-dug wells and boreholes (Oteri et al., 2013). It forms a multi-aquifer system consisting of three aquifer horizons separated by silty and clayey layers (Longe et al., 2011). The Beachline is densely dominated by the Aworis. It is a residential township although it contains some major markets like Alaba international market, Trade fair complex and Iyana-iba market. It also serves as means of transportation for Ferry services and Speed boats.



Figure 1: Lagos state map showing the location of the study area (Omolabi and Adebayo, 2017)

## 2. MATERIALS AND METHODS

### 2.1 Data Acquisition

The geoelectrical resistivity survey was carried out along four traverses (Figure 2) using Pasi 16GL earth resistivity meter, the survey site was geo-referenced with the Garmin global positioning system (GPS) and other accessories used includes four reels of cables, measuring tapes, crocodile clips, battery, four electrodes and hammers. The electrical resistivity method measures the potential differences obtained from artificially-generated electric current introduced into the ground at the surface. Deviations from the pattern of potential differences expected from homogeneous ground provide information on the form of electrical properties of subsurface inhomogeneities (Kearey *et al.*, 2002; Loke 2000). 2D electrical resistivity imaging (ERI) data was acquired using wenner array along the established four traverses (TR1–TR4) of range 85 - 200 m long with inter-electrode

spacings of 10, 20, 30, 40, 50, and 60 m respectively. The electrodes were pegged along the measuring tapes in a straight line, equally spaced and were driven into the soil with the aid of hammers. Each of the four electrode cables was connected to four electrodes with the crocodile clips. The cables were then connected to the resistivity meter powered by a battery, placed at the mid-point. Then, measurements were taken and recorded. The twenty vertical electrical sounding (VES) data was acquired using the Schlumberger array across the four traverses with five VES points on each traverse. For this array, two potentials and two current electrodes were used. The potential electrodes were located within the current electrodes and measuring station was located at the centre of the array. The distance between the current electrodes must be five times greater than or equal to that of the potential electrodes.

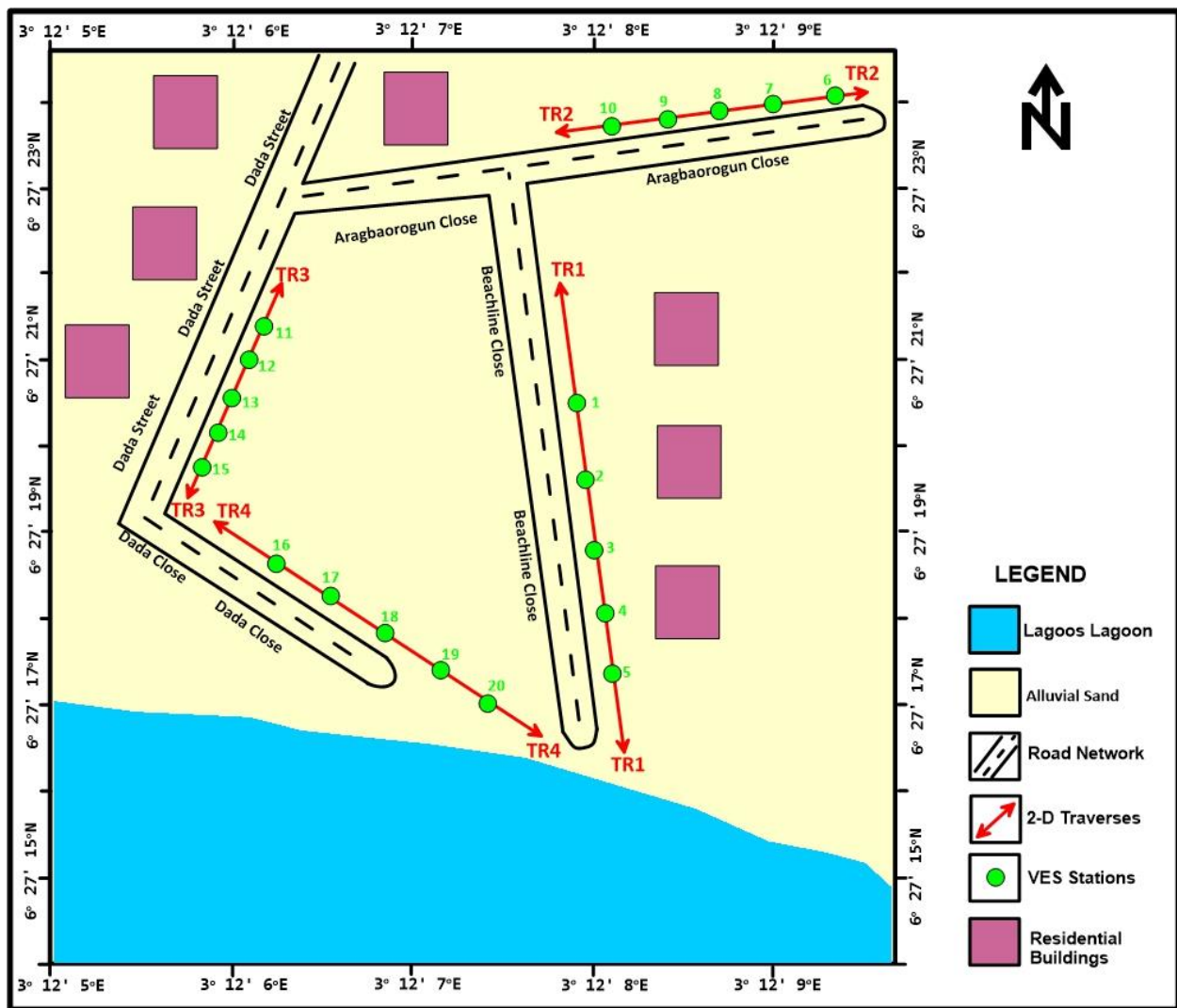


Figure 2: Base map of the study area

## 2.2 Data Processing

The 2D ERI data was processed with the DiproWin software to generate 2D electrical resistivity images revealing the subsurface lateral and vertical resistivity variations while the VES data was plotted on the log-log graph and curve matched with Master and Auxiliary curve types to obtain apparent resistivity values and thicknesses of the subsurface strata (Loke, 2000). These parameters served as input into the WinResist software to generate VES curves. The geoelectric parameters such as thickness, depth, layer and inferred lithology (constrained by borehole data) obtained from the VES curves were in turn used to generate the geoelectric

sections using Surfer version15 software.

## 3. RESULTS AND DISCUSSION

A total spread of 200 m was surveyed, and a depth of 50 m was probed with resistivity values ranging from 3 to 131  $\Omega\text{m}$  along TR1. The 2D ERI (Figure 3a) reveals four geoelectric layers: top soil, sand (saturated with saline water), clay and sandy clay and sand. The resistivity of the topsoil (orange–red colour) varies from 38 to 87  $\Omega\text{m}$ . The sand (saturated with saline water) with resistivity values ranging from 3 to 10  $\Omega\text{m}$  (blue–green colour) is mapped at about 6–15 m. The clay delineated has resistivity values ranging from 17 to 23  $\Omega\text{m}$  (yellow colour) at

depth range 25–30 m. The sandy clay has resistivity range 38 to 58  $\Omega\text{m}$  (red colour) at depth range 30 to 40 m while another sand is delineated with resistivity range (87–131)

$\Omega\text{m}$ . The shallow sand identified in the second layer characterized with low resistivity values (3 to 10)  $\Omega\text{m}$  suggests the infiltration of salt water into the aquifer.

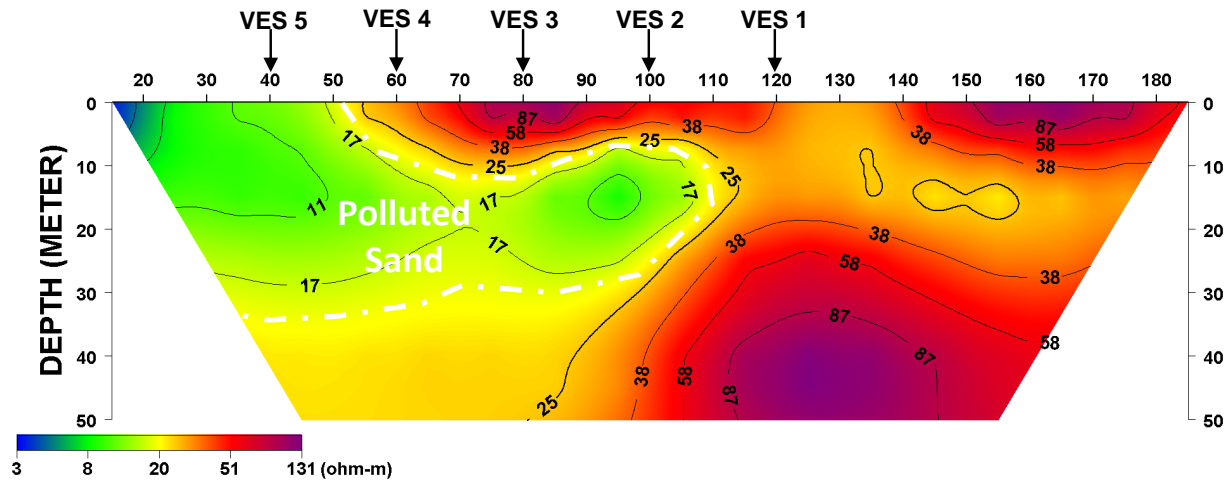


**Figure 3a:** 2-D Resistivity section along TR1

A total spread of 90 m was surveyed, and a depth of 25 m was probed with resistivity values ranging from 25 to 1331  $\Omega\text{m}$  along TR2. The 2D ERI (Figure 3b) reveals four geoelectric layers: topsoil, sand, sandy clay and clay. The resistivity of the topsoil (red–purple colour) varies from 387 to 571  $\Omega\text{m}$ . The sand with resistivity values ranging from 152 to 236  $\Omega\text{m}$  (green–yellow colour) is

mapped at 3–5 m. The sandy clay has resistivity range 63 to 98  $\Omega\text{m}$  (green colour) at depth range 5 to 8 m. The clay delineated has resistivity values ranging from 25 to 40  $\Omega\text{m}$  (blue colour) at depth range 8–25 m. The shallow sand identified in the second layer has not been affected by saltwater intrusion and this could be because it is further away from the beachline.

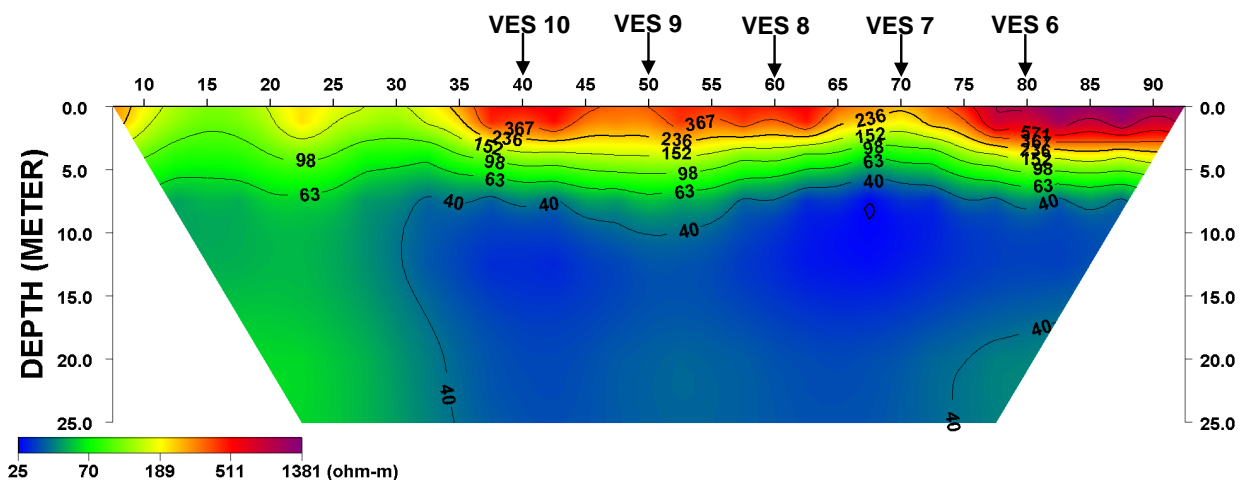


**Figure 3b:** 2-D Resistivity section along TR2



A total spread of 100 m was surveyed, and a depth of 25 m was probed with resistivity values ranging from 1 to 99  $\Omega\text{m}$  along TR3. The 2D ERI (Figure 3c) reveals three geoelectric layers: topsoil, sand (saturated with saline water) and clay. The resistivity of the topsoil (orange–purple colour) varies from 10 to 32  $\Omega\text{m}$ . The sand (saturated with saline water) with resistivity values ranging

from 1.3 to 5.7  $\Omega\text{m}$  (blue–green colour) is mapped at 5–20 m. The clay delineated has resistivity values ranging from 10 to 14  $\Omega\text{m}$  (yellow colour) at depth range 20–25 m. The shallow sand identified in the second layer characterized with low resistivity values (1.3 to 5.7  $\Omega\text{m}$ ) suggests the infiltration of salt water into the aquifer.

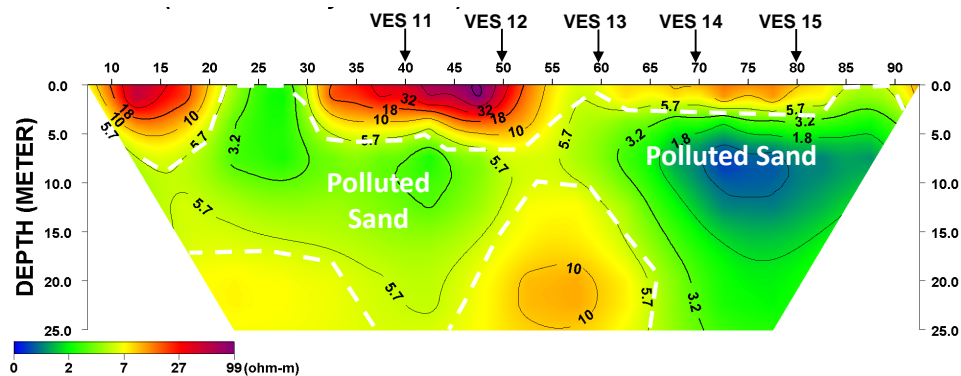
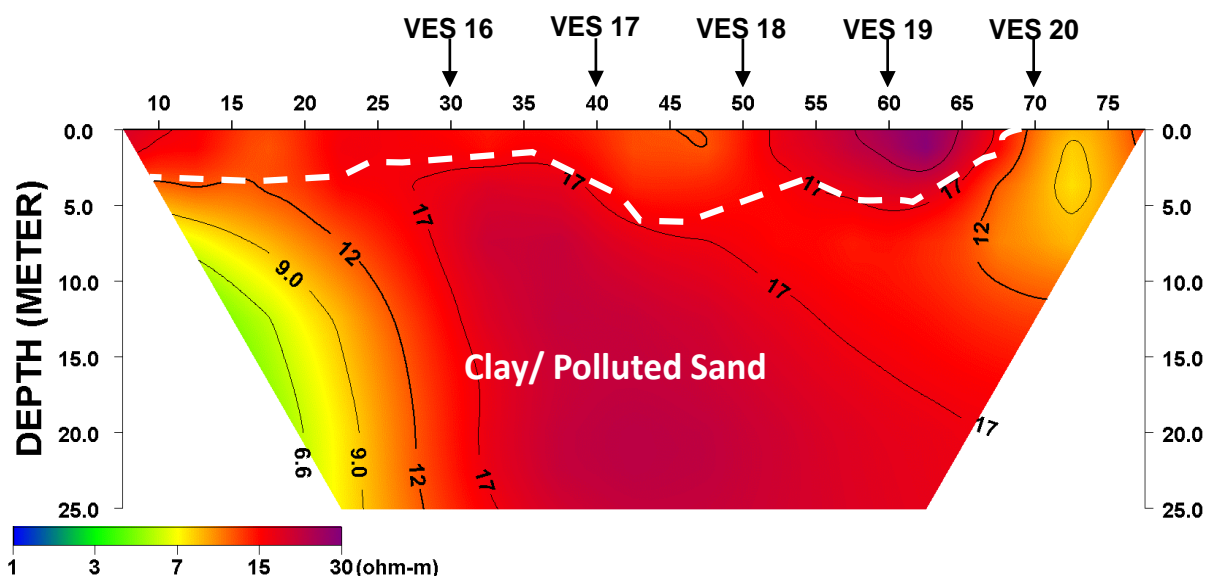


Figure 3c: 2-D Resistivity section along TR3

A total spread of 75 m was surveyed, and a depth of 25 m was probed with resistivity values ranging from 1 to 30  $\Omega\text{m}$  along TR4. The 2D ERI (Figure 3d) reveals three geoelectric layers: topsoil, sand (saturated with saline water) and clay. The resistivity of the topsoil (orange–purple colour) varies from 1 to 17  $\Omega\text{m}$ . The sand (saturated with saline water) with resistivity values ranging

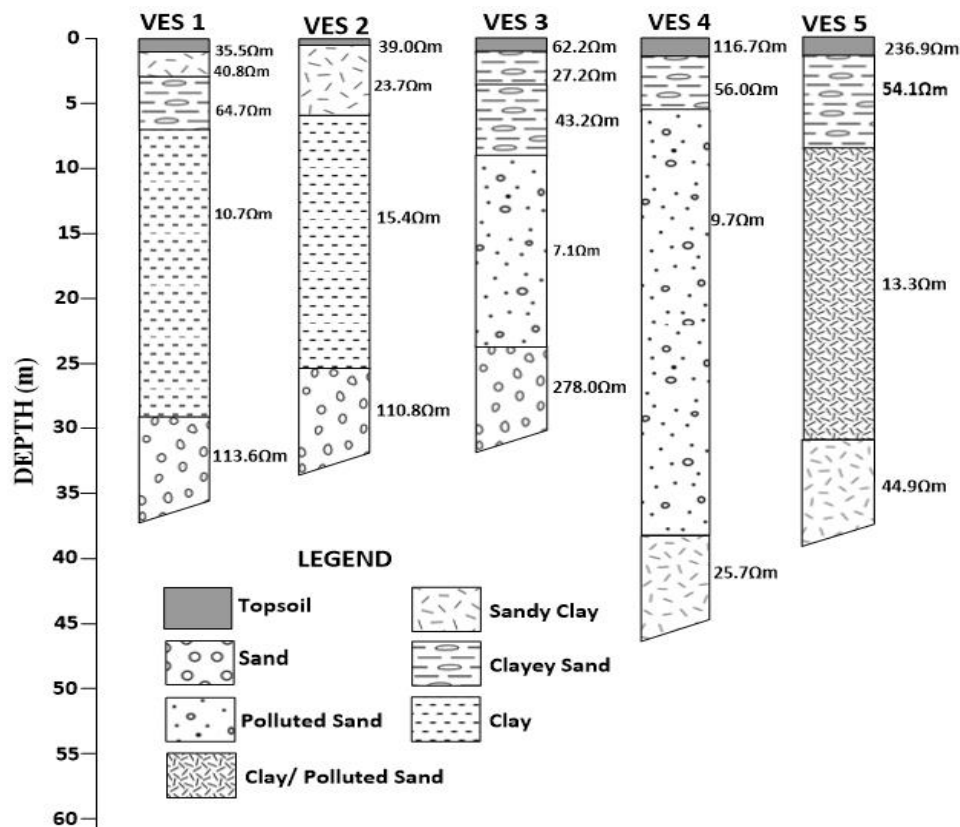
from 6.6 to 9.0  $\Omega\text{m}$  (green colour) is mapped at 5–20 m at lateral distance 10–15 m and 70 to 75 m. The clay delineated has resistivity values ranging from 12 to 17  $\Omega\text{m}$  (red–purple colour) at depth range 20–25 m. The shallow sand identified is characterized with low resistivity values 6.6 to 9.0  $\Omega\text{m}$  which suggests the infiltration of salt water into the aquifer.



**Figure 3d:** 2-D Resistivity Section along TR4

Geoelectric section along TR1 (Figure 3e) shows VES (1– 5) situated at 120, 100, 80, 60, and 40 m respectively. It reveals four to five geo–electric layers ranging from topsoil, clay, clayey sand, sandy clay, sand. The topsoil has resistivity values ranging from 35.5 to 236.9  $\Omega\text{m}$  at depth range 0.5 to 1.3 m. The second layer identified in VES (1 and 2) is sandy clay with resistivity range of 23.7 to 40.8  $\Omega\text{m}$  at depth range 0.5–6 m while the sandy clay is replaced with clayey sand in VES (3-5) with resistivity range 27.2 –56.0  $\Omega\text{m}$  at depth range 1– 10 m. The third layer in VES 1 is clayey sand with resistivity value of 64.7  $\Omega\text{m}$  and layer thickness of 4 m. The third layer in VES (2) is clay with resistivity value 15.4  $\Omega\text{m}$  and layer thickness of 14.2 m. The third layer in VES (3 and 4) comprises of sand (polluted) with resistivity values ranging from 7.1 to 9.7  $\Omega\text{m}$  and at depth range of 5.5 to 40 m respectively. This sand is considered

polluted because of the associated low resistivity which is suggestive of saltwater intrusion. While the third layer in VES (5) denotes clay/polluted sand having resistivity value of 13.3  $\Omega\text{m}$  and thickness value of 24 m. The fourth layer identified in VES (1) denotes clay with resistivity value of 10.7  $\Omega\text{m}$  and layer thickness 18 m where the clay is replaced with sand in VES (2 and 3) with resistivity range 110.8 –278  $\Omega\text{m}$  at depth range of 24.1 m. The fourth layer in VES 4 is sandy clay with resistivity value 25.7  $\Omega\text{m}$ . Also, the fourth layer in VES 5 indicates sandy clay with resistivity value of 44.9  $\Omega\text{m}$  but its thickness could not be determined as a result of loss of current. The fifth horizon in VES (1) is indicative of sand with no thickness due to its current loss in the region. The sand in the fifth and fourth layer of VES 1 and VES 2 respectively is a confined aquifer where groundwater could be tapped.

**Figure 3e:** Geoelectric section along TR1

Geoelectric section along T2 (Figure 3f) shows VES (6–10) situated at 80, 70, 60, 50, and 40 m respectively. It reveals four to five geo-electric layers ranging from topsoil, clay, clayey sand, sandy clay, sand. The topsoil has resistivity values ranging from 295.7 to 720.7  $\Omega\text{m}$  at depth range 0.5 to 2.5 m. The second layer identified across VES (6–10) is sand with resistivity range of 110.0 to 694.5  $\Omega\text{m}$  at depth range 4.0–8.0 m. The third layer in VES 6 is clay with resistivity value of 25.5  $\Omega\text{m}$  with layer thickness of 40 m. The third layer in VES (7 and 9) is sandy clay with resistivity range 38.9–41.8  $\Omega\text{m}$  at depth range of 15–20 m. The third layer in VES (8) is clay having resistivity 23.6  $\Omega\text{m}$  and layer thickness of 4 m. The third layer in VES 10 is clayey sand having resistivity value of 34.5  $\Omega\text{m}$  and thickness 30 m. The fourth layer in VES 6 is sandy clay with resistivity value

49.2  $\Omega\text{m}$  but its thickness could not be determined because of loss of current while the fourth layer in VES 7 indicates clay with resistivity value of 16.0  $\Omega\text{m}$  with layer thickness of about 24 m. The fourth layer in VES (8 and 10) is sand with resistivity range of 113.7 to 121.7 with depth range 14–32 m for VES 8 while the thickness of VES 10 could not be ascertained due to current termination at this zone. The sand identified in the fourth layer (VES 8) is a confined aquifer where ground water could be exploited. The fifth horizon in VES (7) is indicative of clayey sand having resistivity value 49.5  $\Omega\text{m}$  with no thickness due to its current loss in the region. The fifth layer in VES (8) denotes clay with resistivity value 23.5  $\Omega\text{m}$  but its thickness could not be determined as a result of loss of current.

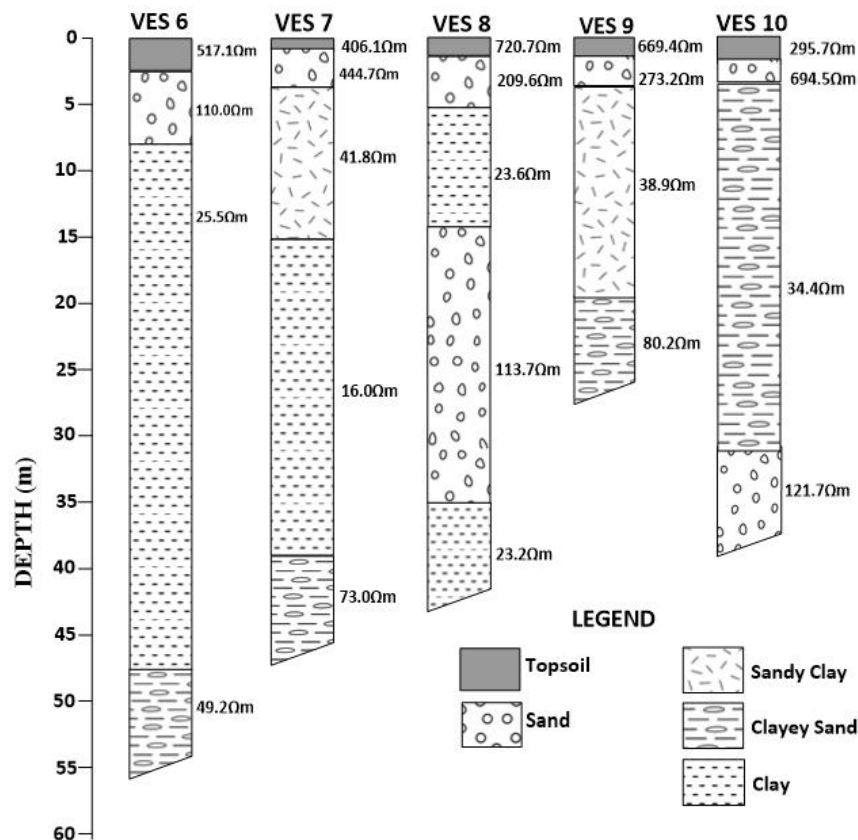


**Figure 3f:** Geoelectric section along TR2



Geoelectric section along TR3 (Figure 3g) shows VES (11–15) situated at 40, 50, 60, 70, and 80 m respectively. It reveals four geoelectric layers ranging from topsoil, clayey sand, sandy clay, and sand. The topsoil has resistivity values ranging from 53.2 to 138.2  $\Omega\text{m}$  at depth range 0.5 to 1.3 m. The second layer identified in VES (11) is sand with resistivity value of 9.1  $\Omega\text{m}$  at depth range 0.5–8 m while the sand is replaced with sandy clay in VES (12–14) with resistivity range 17.6–28.6  $\Omega\text{m}$  at depth range 1–4 m. The third layer in VES (11–13) is sand (polluted) with resistivity range of 1.3–10.6  $\Omega\text{m}$  at depth range of 4–44m. The third layer in VES (14) denotes sandy clay with resistivity value

33.3  $\Omega\text{m}$  and layer thickness of 31.2 m. The third layer in VES (15) comprises of clayey sand with resistivity value of 66.8  $\Omega\text{m}$  and thickness of about 15m. This sand is considered polluted because of the associated low resistivity which is suggestive of saltwater intrusion. The fourth layer identified in VES (11) denotes sand (polluted) with resistivity value of 3.2  $\Omega\text{m}$ , where the sand is replaced with clay in VES (12, 14 and 15) with resistivity range 23.1–26.0  $\Omega\text{m}$  and clayey sand in identified in VES (13) with resistivity value 82.0  $\Omega\text{m}$  but their respective thicknesses could not be determined as a result of loss of current in this zone.

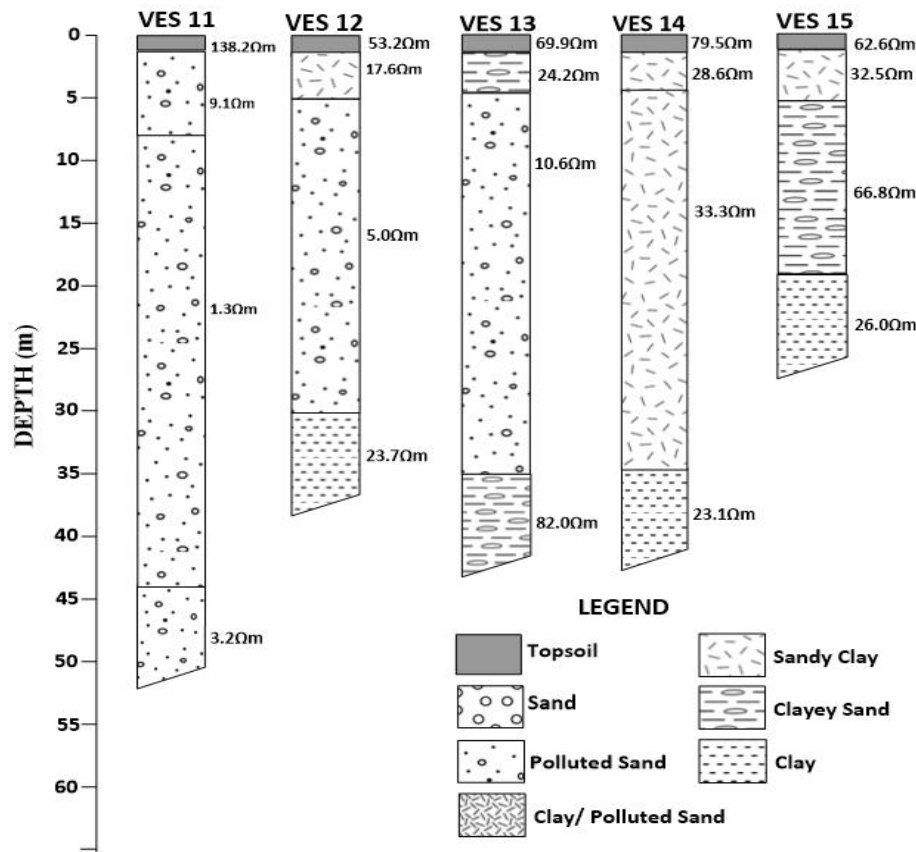


Figure 3g: Geoelectric section along TR3

Geoelectric section along TR4 (Figure 3h) shows VES (16–20) situated at 30, 40, 50, 60, and 70 m respectively. It reveals four to five geoelectric layers ranging from topsoil, clay, clayey sand, sandy clay, sand. The topsoil has resistivity ranging from 9.8 to 135.0  $\Omega\text{m}$  at

depth range 0.2 to 2.3 m. The second layer identified in VES (16) is sand with resistivity value of 103.6 with thickness of about 5 m while the sand is replaced with sandy clay in VES (17) with resistivity value 43.6  $\Omega\text{m}$  with layer thickness 6.5 m. The second layer in

VES (18–20) is clayey sand with resistivity range 64.3–79.3  $\Omega\text{m}$  at depth range 2.3–10 m. The third layer in VES (16 and 17) is clay with resistivity range 25.1–28.0  $\Omega\text{m}$  at depth range of 10–22 m. The third layer in VES (18 and 19) comprises of sand (polluted) with resistivity ranging from 4.5–7.1  $\Omega\text{m}$  and at depth range of 26 to 38 m. This sand is considered polluted because of the associated low resistivity which is suggestive of saltwater intrusion. While the third layer in VES (20) denotes clay/polluted sand having resistivity value of 12.7  $\Omega\text{m}$  and thickness value of 21 m. The fourth layer identified in

VES (16 and 20) denotes sand with resistivity value of 100.5–154.1  $\Omega\text{m}$  though the thickness could not be ascertained due to current termination at this zone. The sand identified in fourth layer VES (16) is a confined aquifer that could be explored for groundwater exploration. The fourth layer in VES (17 and 18) is clay having resistivity range 12.4–30.5  $\Omega\text{m}$  while clayey sand is identified in VES (19) with resistivity value of 40  $\Omega\text{m}$  but their respective thicknesses could not be determined as a result of loss of current at this zone.

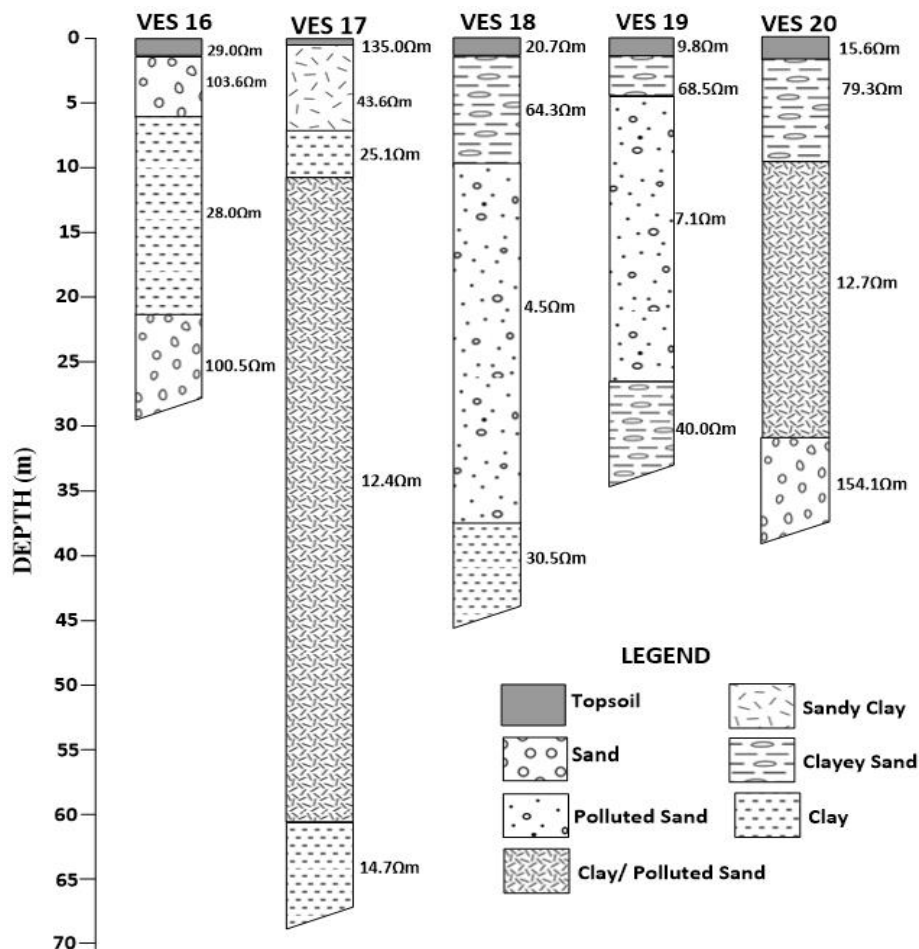
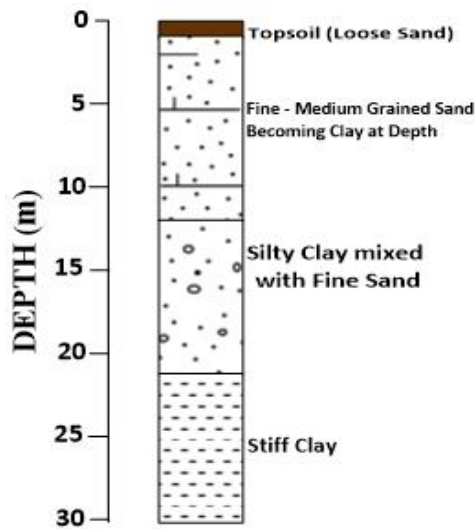


Figure 3h: Geoelectric section along TR4



**Figure 3i:** The borehole (BH) data modified from Ayolabi and Adegbola (2013)

#### 4. CONCLUSION

The assessment of saltwater intrusion into the coastal aquifer using electrical resistivity method was conducted along the coastline Ojo, Lagos state with a view locating possible regions for groundwater exploration. The sand delineated in the second layer of the 2D electrical resistivity images across TR (1, 3 and 4) with low resistivity response revealed the lateral and vertical extent of contamination which also coincided with the anomaly observed in the VES results. The interpretation of results was guided by obtained borehole data and results from the control profile. The sand identified in the second and third layers along TR1 (VES 3 and 4), TR3 (VES 11–13) and TR4 (VES 18 and 19) with low resistivity values of range 1.3–10.6  $\Omega\text{m}$  at depth range 0.5–44 m showed the relative degree of saltwater intrusion when compared to the identified sand in TR2 2D ERI away from the Beachline (control profile). However, a probable confined freshwater aquifer with resistivity range 100.5–278  $\Omega\text{m}$  for VES (1 and 2) along TR1, VES (16) along TR4 at depth 30 m and VES (8) along TR2 at depth range

14–32 m was identified at fourth and fifth geoelectric layers. This confined aquifer could be considered for groundwater exploration. Hence, it is imperative to monitor the saline contamination so as to preserve the quality of groundwater in the study area.

#### Conflict of Interest

The authors declare that there is no conflict of interest.

#### Acknowledgments

The Authors would like to appreciate Earth Signature Research Group (ESREG) for the manuscript review.

#### REFERENCES

- Ahmed Al, B. and Tariq, H., (2006). Sea Water Intrusion in a Coastal Aquifer: A Case Study for the Area Between Seeb and Suwaiq, Sultanate of Oman. *Agricultural and Marine Sciences*, 11: 55-69
- Adeogun, O. Y., Adeoti, L., Jimoh, M. M., Adegbola, R. B., Oyeniran, T. A., and Alli, S. A., (2019). Integrated approach for groundwater assessment in Yetunde Brown, Ifako, Gbagada, Lagos State, Nigeria. *Journal of*

- Applied Sciences and Environmental Management*, 23(4): 593-602.
- Adeoti, L., Alile, O., and Uchegbulam, O., (2010). Geophysical investigation of saline water intrusion into freshwater aquifers: A case study of Oniru, Lagos State. *Scientific Research and Essays*. 5:248-259.
- Adepelumi, A. A., Ako, B. D., Ajayi, T. R., Olorunfemi, A. O., Awoyemi, M. O., and Falebita, D. E., (2008). Integrated geophysical mapping of the Ifewara transcurrent fault system, Nigeria. *Journal of African Earth Sciences*, 52(4-5): 161-166.
- Adepelumi, A. A., Olorunfemi, M. O., Falebita, D. E., and Bayowa, O. G., (2009). Structural mapping of coastal plain sands using engineering geophysical technique: Lagos Nigeria Case Study. *Natural Science*, 1(1): 2-9.
- Alabi, A. A., Ogungbe, A. and Oyerinde, H.O. (2010). Determination of groundwater potential in Lagos State University, Ojo: using geoelectric methods (Vertical electrical sounding and horizontal profiling) *Unpublished*.
- Ayolabi, E.A., Folorunso, A.F., Odukoya, A.M., Kayode, O.T., (2013). Mapping saline water intrusion into the coastal aquifer with geophysical and geochemical techniques: the University of Lagos campus case (Nigeria). Springer Plus 2, 433.<https://doi.org/10.1186/2193-1801-2-433>
- Ayolabi, E. A. and Adegbola, R. B., (2014). Application of MASW in road failure investigation. *Arabian Journal of Geosciences*, 7(10): 4335-4341.
- [Bellafiore](#), D., [Ferrarin](#), C., [Maicu](#), F., [Manfè](#), G., [Lorenzetti](#), G., [Umgiesser](#), G., [Zaggia](#), L., [Levinson](#), A.V. (2021). Saltwater intrusion in a mediterranean delta under a changing Climate. *Journal of Geophysical Research: Ocean*, 126, (2) <https://doi.org/10.1029/2020JC01643>
- [7](#)  
Cong-Thi, D., Dieu, L.P., Thibaut, R., Paepen, M., Ho, H.H., Nguyen, F. and Hermans, T., (2021). Imaging the Structure and the Saltwater Intrusion Extent of the Luy River Coastal Aquifer (Binh Thuan, Vietnam) Using Electrical Resistivity Tomography. *Water*, 13, 1743 <https://doi.org/10.3390/w13131743>.
- Herbert, E. R., Boon, P., Burgin, A. J., Neubauer, S. C., Franklin, R. B., Ardón, M., Hopfensperger, K.N., Lamers, L.P.M. and Gell, P. (2015). A global perspective on wetland salinization: ecological consequences of a growing threat to freshwater wetlands. *Ecosphere*, 6(10): 1-43.
- Hinrichsen, H.H., Lehmann, A., Petereit, C., Schmidt, J. (2007). Correlation analyses of Baltic Sea winter water mass formation and its impact on secondary and tertiary production, *Oceanologia*, 49 (3):381-395.
- Kearey, P., Brooks, M. M. and Hill, I., (2002). *An Introduction to Geophysical Exploration*. Third Edition, Blackwell, London.262
- Khalil, M.H., (2006). Geoelectric resistivity sounding for delineating saltwater intrusion in the Abu Zenima area, west Sinai, Egypt, *Journal of Geophysics and Engineering*, 3: 243–251
- Loke, M., (2000). *Electrical Imaging Surveys for Environmental and Engineering Studies. A Practical Guide to 2-D and 3-D surveys*, Heritage Geophysics.11-65
- Longe, E. O., (2011). Groundwater resources potential in the coastal plain sands' aquifers, Lagos, Nigeria. *Research Journal of Environmental and Earth Sciences*, 3(1): 1-7.
- Manivannan, V. and Elango, L., (2019). Seawater intrusion and submarine

- groundwater discharge along the Indian coast. *Environmental Science and Pollution Research*, 26(31), 31592-31608.
- Oladapo, M.I., Ilori, O.B. and Adewoye-Oladapo, O.O., (2014). Geophysical Study of saline water intrusion in Lagos municipality. *African Journal of Environmental Science and Technology* 8 (1): 16 – 30
- Omolabi, A. O. and Adebayo, P. W., (2017). An assessment of the housing policy performance towards public low-income housing provision and management in Lagos, Nigeria. *International Journal of Development and Sustainability*, 6(8):792-809.
- Oteri, A. U. and Atolagbe, F. P., (2003, March). Saltwater intrusion into coastal aquifers in Nigeria. In *the Second International Conference on Saltwater Intrusion and Coastal Aquifer-Monitoring, Modeling, and Management. Mirada, Yucatan, Mexico*.
- Oteri, A.U., (2013) Unpublished work Presentation on Coastal groundwater resource—Abstraction, Quality and Related Environment Concerns: Lagos State Case Study. Lagos State Water Regulatory Commission [LSWRC] Workshop June 2013-Groundwater Resources of Lagos State.
- Richter, B.C. and Kreitler, C.W., (1993). *Geochemical Techniques for Identifying Sources of Ground-water Salinization*. CRC Press.
- Robinson, G.A., Ahmed, A.A. and Hamil, G.A., (2016). Experimental saltwater intrusion in coastal aquifers using automated image analysis: application to the homogeneous aquifer. *Journal of Hydrology*, 538: 304-313
- Satriani A., Loperte A., Imbrenda V., and Lapenna V., (2012). Geoelectrical Surveys for Characterization of the Coastal Saltwater Intrusion in Metapontum Forest Reserve (Southern Italy). *International Journal of Geophysics*, 238478:1-8 doi:10.1155/2012/238478
- Tomaszkiewicz, M., Abou Najm, M., and El-Fadel, M., (2014). Development of a groundwater quality index for seawater intrusion in coastal aquifers. *Environmental Modelling & Software*, 57:13-26.  
<https://doi.org/10.1016/j.envsoft.2014.03.010>
- Werner, A.D. and Simmons, C.T. (2009). Impact of Sea-Level Rise on Sea Water Intrusion in Coastal Aquifers. *Groundwater*, 47, 197-204. <https://doi.org/10.1111/j.1745-6584.2008.00535.x>



